Distributed Rigidity-Based Active Localization for Heterogeneous Teams

Federico Oliva*, Ido Sherf, and Amir Degani

CEAR Lab, Technion - Israel Institute of Technology
*federicoo@campus.technion.ac.il

Abstract. This work proposes a distributed rigidity-based Active localization policy for a heterogeneous team structured with a leader and a set of children, all provided with ranging sensors. Considering an unknown environment, we first exploit Rigidity Theory to develop a motion policy such that all the agents can recover their position with respect to the leader. Furthermore, we propose a geometrical interpretation of rigidity, maximizing the team's exploration capabilities.

1 Introduction

Recently, increasing interest has been drawn to collaborative robotics, specifically in heterogeneous multi-agent systems (MAS) [1]; these are characterized by agents differing in cognitive or physical properties, typically operating in unknown environments [2, 3]. In these scenarios, collaborative exploration becomes a fundamental task, mainly addressed through *Simultaneous Localization And Mapping* (SLAM) [4–7], Bayesian filtering-based, and distributed localization solutions [8–11]. The sensor setup usually considers bearing and distance measurements, both in *Line of Sight* (LOS) and *Non-Line of Sight* (NLOS) conditions [12–15].

In this context, Active localization arises as a valid methodology [16, 17]; it consists of a decision-making process in which each agent chooses its future control actions, balancing exploring new areas and exploiting those already seen to improve localization; it dates back to the 90s, with the *Cooperative Positioning System* (CPS) proposed by Hirose and Kurazume [18–22].

Among the proposed Active localization approaches, in this work, we focus on those exploiting *Rigidity Theory*; it consists of a mathematical framework hinged on *Graph Theory* that can be used to find the conditions for unique localizability of a network whose agents are provided with distances from their neighbors [23–26]. Extensions have been developed exploiting bearing measurements [27–30].

1.1 Related work and contributions

This work considers a heterogeneous team with a leader and a set of children, as in [18], and focuses on two main aspects: network localization and environment mapping coverage [31–34]. We now proceed to describe those previous works that inspired our research and outline our main contributions.

Network localization Rigidity Theory provides conditions to unambiguously locate all nodes in a positioned network, depending on the connectivity properties of its communication graph. In Active localization, agents not satisfying such conditions are provided with a motion policy that increases their chances of recovering them. Shames [35] considers a team of agents exploring an unknown environment scattered with fixed landmarks with unknown locations. Each agent detects a set of landmarks and shares them with any neighbor. Rigidity Theory is exploited to find the conditions under which agents can merge their local maps, embedding them as constraints in the exploring actions. In the first part of this work, we develop a distributed rigidity-based localization algorithm, relaxing the assumptions from [35]; we localize the entire team with respect to the leader, starting from a non-rigid and simply connected network. Most importantly, the proposed algorithm is modular, allowing us to expand the goals of the motion policy to the team mapping coverage.

Mapping coverage The second part of this work interprets the concept of rigidity in terms of the agents' spatial disposition and, in particular, dispersion, connectivity, and symmetry. The goal is to define a rigidity-based cost function to embed in our previous algorithm, allowing the team to localize and best explore the surroundings. In this sense, we were inspired by two works, one by Zhu [36] and the other by Zelazo [37], which we integrate linking rigidity to coverage.

1.2 Structure and notation

The work is structured as follows: first, the considered case study is described in section 2. Secondly, the fundamentals of Rigidity Theory are recalled in section 3. The work then details the two main contributions: the rigidity-based distributed Active localization algorithm in section 4 and the rigidity spatial interpretation in section 5. Conclusions and future research directions are drawn in section 6.

Notation Vector quantities are described by bold lowercase letters. Symbols (μ, σ) refer to mean and standard deviation. $\|\cdot\|$ defines the 2-norm operator. $\dot{x}$ refers to the time derivative of x. The matrix operator $\sigma(\mathbf{M})$ of a generic square matrix $\mathbf{M}$ returns its set of eigenvalues, i.e., its spectrum. We refer to a ball centered in $\boldsymbol{x}_0 \in \mathbb{R}^n$ with radius $\epsilon > 0$ as the set $\mathcal{B}_\epsilon(\boldsymbol{x}_0) \triangleq \{\boldsymbol{x} \in \mathbb{R}^n \text{ s.t. } \|\boldsymbol{x} - \boldsymbol{x}_0\| < \epsilon\}$. Graphs will be referred to with the calligraphic letter $\mathcal{G}$. The set of nodes and edges in $\mathcal{G}$ are $\mathcal{V}$ and $\mathcal{E}$, respectively, and $|\mathcal{V}| = n$ and $|\mathcal{E}| = m$ are their cardinalities. In this work, we consider undirected graphs, i.e., $(i,j) \in \mathcal{E} \iff (j,i) \in \mathcal{E}$. Thus, for a generic agent A_i, the set of neighbors is $\mathcal{N}_i \triangleq \{j \in \mathcal{V} \text{ s.t. } (i,j) \in \mathcal{E}\}$. The $\sim$ before a logical condition describes its negation.

2 Problem statement

Consider a team of agents on a 2D map; the team is split into a leader A_L and the remaining children. Every agent has a range sensor (e.g., UWB antennas) with a sensing limit $\delta = 8$m. The team leader is additionally provided with a vision system with a FOV and a maximum distance of $\delta_C = 3$m; each agent

falling within the camera's FOV is localized in the leader's reference frame. The agents are also provided with environment mapping sensors (e.g., wide-angle cameras, air quality sensors, etc.) with maximum range $\delta_M = 3$m. A graphic representation of the model is depicted in fig. 1[1].

In this work, we consider a noise-free scenario. However, this model aims to describe a heterogeneous team where only the leader is provided with accurate (and more expensive) sensing technology, while all the other agents can only rely on higher-noise COTS sensors. Given this setup, we now define the two problems addressed in this work: the network localization problem and the environment coverage problem.

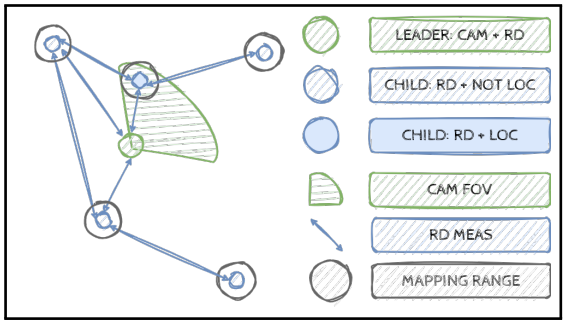

Fig. 1: Graphic representation of our case study. RD stands for *Relative Distance*, LOC for *Localized*.

The network localization problem We want to localize all the children with respect to the leader. This problem can be modeled through a framework, i.e., a positioned graph. For a team with agents' positions $\boldsymbol{p} = \{\boldsymbol{p}_i\}$ and communication graph $\mathcal{G}$ defined by the ranging sensors, the related framework is the pair $(\mathcal{G}, \boldsymbol{p})$. Every localized agent is called a *beacon* node. Beacons are a subset of the agents' set, i.e., $n_b < n$. With this notation, we define the following problem:

Problem 1 (Network localization problem). The network localization problem with distance information consists in unambiguously determining the locations $\boldsymbol{p}_i \in \boldsymbol{p}$ of framework $(\mathcal{G}, \boldsymbol{p})$, given the positions of the beacon nodes, and the distances among neighbors.

The environment coverage problem We define the mapping area of agent i as $M_i = \pi\delta_M^2$. Indeed, when $\|\boldsymbol{p}_i - \boldsymbol{p}_j\| < 2\delta_M$, the two mapping areas have an overlap I_{ij}. With this notation, we define the following problem:

Problem 2 (Environment coverage problem). The environment coverage problem for a localized heterogeneous team described by a generic framework $(\mathcal{G}, \boldsymbol{p})$ consists of maximizing the static team coverage, which is defined as

$$\mathcal{C} \triangleq \frac{\sum_{i=1}^{n} \left(M_i - \sum_{j \in \mathcal{N}_i} I_{ij} \right)}{A_{\text{env}}}, \tag{1}$$

where A_{env} represents the total area of the environment.

[1]The distances in the figure are not correctly scaled.

3 Rigidity Theory

This section recalls the main concepts and results of the Rigidity Theory for distance-based network localization [23–25,37]. As introduced in section 1, Rigidity Theory deals with agents' positions and connectivity; thus, it is well-described through frameworks. The two framework properties fundamental to rigidity are *equivalence* and *congruence*. Two frameworks $(\mathcal{G}, \boldsymbol{p}_0)$ and $(\mathcal{G}, \boldsymbol{p}_1)$ are *equivalent* when all their edges' lengths are equal, while they are *congruent* when this is true for all the node's distances. Consider fig. 2a for an example. For a graph $\mathcal{G}$, all the frameworks equivalent up to isometric transformations are called *realizations*. When only one framework realization exists, the network localization problem can be *unambiguously* solved. We now introduce rigidity:

Definition 1 ((Infinitesimal) Rigidity). *A framework $(\mathcal{G}, \boldsymbol{p}_0)$ is rigid there exists an $\epsilon > 0$ such that every framework $(\mathcal{G}, \boldsymbol{p}_1)$ which is equivalent to $(\mathcal{G}, \boldsymbol{p}_0)$ and satisfies $\|\boldsymbol{p}_{0,i} - \boldsymbol{p}_{1,i}\| < \epsilon \ \forall i \in \mathcal{V}$, is congruent to $(\mathcal{G}, \boldsymbol{p}_0)$.*

Rigidity can be seen as the capability of a framework to maintain congruence when equivalence-keeping transformations are applied with displacements limited to a ball $\mathcal{B}_\epsilon(\boldsymbol{p}_i)$ for each node (i.e., local behavior). If we consider any edge $(i, j) \in \mathcal{E}$, the following holds for a generic framework $(\mathcal{G}, \boldsymbol{p})$:

$$(\boldsymbol{p}_i - \boldsymbol{p}_j)^T (\boldsymbol{p}_i - \boldsymbol{p}_j) = d_{ij}^2, \tag{2}$$

with d_{ij} the distance between nodes. To investigate the infinitesimal motions of a framework, we study the local behavior of the solutions to (2) through its tangent space:

$$(\boldsymbol{p}_i - \boldsymbol{p}_j)^T (\dot{\boldsymbol{p}}_i - \dot{\boldsymbol{p}}_j) = 0 \implies \mathcal{R}(\mathcal{G}, \boldsymbol{p}) \dot{\boldsymbol{p}} = 0, \tag{3}$$

where $\mathcal{R} \in \mathbb{R}^{m \times 2n}$ is called *rigidity matrix* [24]. Each row of $\mathcal{R}$ represents an edge, and it is structured as follows:

$$\mathcal{R}(\mathcal{G}, \boldsymbol{p})_{ij, i<j} = \Big[\underbrace{\mathbf{0}}_{1 \dots 2(i-1)} \ (\boldsymbol{p}_i - \boldsymbol{p}_j)^T \ \underbrace{\mathbf{0}}_{2(i+1) \dots 2(j-1)} \ (\boldsymbol{p}_j - \boldsymbol{p}_i)^T \ \underbrace{\mathbf{0}}_{2(j+1) \dots 2n} \Big]. \tag{4}$$

The rigidity matrix is of great help in assessing infinitesimal rigidity [24]:

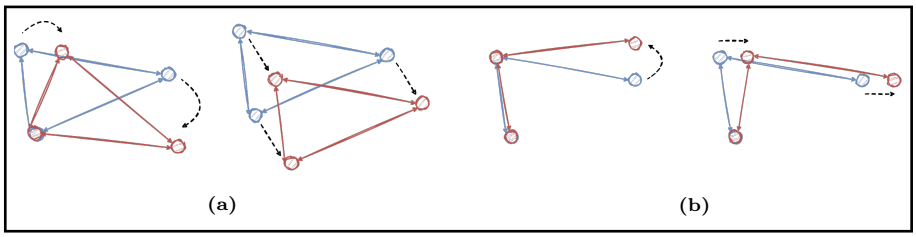

Fig. 2: (a) the blue framework can be transformed through rotations and translations (i.e., isometric transformations) without affecting the edges' length or the nodes' distances. (b) this is not true here, where equivalence is maintained but not congruence.

Lemma 1 (Rigidity matrix rank). *A framework* $(\mathcal{G}, \boldsymbol{p})$ *in* $\mathbb{R}^2$ *infinitesimally rigid if and only if* $\texttt{rank}(\mathcal{R}(\mathcal{G}, \boldsymbol{p})) = 2n - 3$.

Moore [38] states that "non-rigid graphs can be continuously deformed to produce an infinite number of realizations." Thus, rigid graphs can't be *continuously* deformed, but still have *discontinuous* deformations that can prevent a realization from being unique[2]. Consequently, infinitesimal rigidity can't be used as a sufficient condition for the unicity of a framework realization. A more strict condition is needed, i.e., global rigidity:

Definition 2 (Global rigidity). *A framework* $(\mathcal{G}, \boldsymbol{p}_0)$ *is globally rigid if every framework which is equivalent to* $(\mathcal{G}, \boldsymbol{p}_0)$*, is also congruent to* $(\mathcal{G}, \boldsymbol{p}_0)$.

Global rigidity is related to frameworks' unique realizations ([24] [Theorem 1]):

Theorem 1. *Consider a framework* $(\mathcal{G}, \boldsymbol{p})$ *in* $\mathbb{R}^2$*, with* $n_b \geq 3$ *beacon nodes placed at* $p_b = \{\boldsymbol{p}_1 \ \dots \ \boldsymbol{p}_{n_b}\} \subset \boldsymbol{p}$ *and* $n - n_b$ *ordinary nodes placed at* $p_o = \{\boldsymbol{p}_{n_b+1} \ \dots \ \boldsymbol{p}_n\} \subset \boldsymbol{p}$*. We also assume that at least three beacons are not aligned. Then, the network localization problem is solvable if and only if the framework* $(\mathcal{G}, \boldsymbol{p})$ *is globally rigid.*

The global rigidity and beacon alignment conditions in theorem 1 address the network's spatial disposition and connectivity, characterizing the framework's two constructive entities, i.e., the graph $\mathcal{G}$ and the positions $\boldsymbol{p}$. Constructive conditions to check global rigidity on the plane are provided in [24] [Theorem 6]:

Theorem 2. *A graph* $\mathcal{G}$ *with* $n \geq 4$ *vertices is generically globally rigid in* $\mathbb{R}^2$ *if and only if it is 3-connected and redundantly rigid in* $\mathbb{R}^2$.

Here, *generic global rigidity* refers to globally rigid frameworks robust to small perturbations. Moreover, *3-connectivity* refers to graphs that remain connected after removing any pair of nodes. *Redundant rigidity* refers to frameworks that remain infinitesimally rigid after removing any single edge. We are left with three constructive conditions to check whether the localization problem can be unambiguously solved: beacon alignment, 3-connectivity, and redundant rigidity. We will use these in our distributed Active localization algorithm, which will be presented in the next section.

4 Distributed Active localization

In this section, we address the network localization problem stated in section 2, proposing a distributed heuristic algorithm based on the results from section 3.

4.1 The algorithm

We focused on two goals: keeping the assumptions on the initial network configuration as general as possible and the distributed structure of the algorithm. Thus, we structured the algorithm in three actions, which are asynchronously repeated by every agent A_i:

[2] See [38], and specifically *flip ambiguities* and *discontinuous flex ambiguities*.

- `GetNeighbors`: A_i collects all the measurements in a `LOStable`. Ranging sensors provide each agent with the ID and distance of other agents within δ, defining $\mathcal{N}_{i,RD}$. When A_i is the leader, the camera provides children's ID, distance, and bearing (i.e., position) within δ_C, defining $\mathcal{N}_{L,CAM}$.
- `GetPosition`: the information from `LOStable` is combined with theorem 1 and theorem 2, checking the node's localizability.
- `MovePolicy`: if `GetPosition` couldn't positively assess the localizability of A_i, the agent moves accordingly to a heuristic policy aiming to increase the chances to become so in the next iteration.

Let's look at algorithm 1 for more details on `GetPosition`; we define $\overline{\mathcal{N}}_{i,RD}$ as the subset of localized agents from $\mathcal{N}_{i,RD}$ with at least three non-aligned elements. After checking the most trivial conditions as being localized by the leader or not having the minimum number of localized neighbors (CFR. theorem 1), A_i selects only the `LOStable` entries referring to $\overline{\mathcal{N}}_{i,RD}$, creating a framework $\mathcal{F}$ (CFR. A_i.`BuildFrameWork`). Theorem 2 conditions are checked on $\mathcal{F}$; if they are not satisfied, agents are removed from $\mathcal{F}$ until the largest globally rigid sub-framework $\mathcal{F}^*$ is found (CFR. A_i.`ReduceFrameWork`). When a globally rigid framework is found, the agent is localized by solving a trilateration problem.

Algorithm 1 `GetPosition`

function GetPosition(A_i)
  if $A_i = A_L \mid A_i \in \mathcal{N}_{L,CAM}$ **then** A_i.`localized` $\leftarrow$ `true`
    return
  end if
  if $|\overline{\mathcal{N}}_{i,RD}| < 3$ **then** A_i.`localized` $\leftarrow$ `false`
    return
  end if
  $\mathcal{F} \leftarrow A_i$.`BuildFrameWork`$(\overline{\mathcal{N}}_{i,RD})$
  if Is3Connected($\mathcal{F}$) & IsRedundant($\mathcal{F}$) **then** A_i.`localized` $\leftarrow$ `true`
  else
    do $(\mathcal{F}^*, \overline{\mathcal{N}}^*_{i,RD}) \leftarrow A_i$.`ReduceFrameWork`$(\mathcal{F})$
    while ($\sim$Is3Connected($\mathcal{F}^*$) & $\sim$IsRedundant($\mathcal{F}^*$)) | ($|\overline{\mathcal{N}}^*_{i,RD}| < 3$)
    if Is3Connected($\mathcal{F}^*$) & IsRedundant($\mathcal{F}^*$) & ($|\overline{\mathcal{N}}^*_{i,RD}| \geq 3$) **then**
      A_i.`localized` $\leftarrow$ `true`
    else
      A_i.`localized` $\leftarrow$ `false`
    end if
  end if
end function

If A_i can't localize itself through `GetPosition`, as long as $\mathcal{N}_{i,RD} \neq \emptyset$, it can move towards its neighbors; by doing so, the chances of either increasing $|\mathcal{N}_{i,RD}|$ or falling within $\mathcal{N}_{L,CAM}$ get higher. The idea behind the heuristic `MovePolicy` (CFR. algorithm 2) is to numerically compute the gradient of the measured distances' average by moving A_i of ϵ on the four points [$\pm\epsilon$, $\pm\epsilon$] (CFR. A_i.`DistGrad`). If A_i has localized neighbors, they are the only ones used to

compute the gradient. Otherwise, all the neighbors are considered. The point with the lowest measured distances' average is selected as the next A_i's motion $\boldsymbol{v}$. Lastly, A_i actuates $\boldsymbol{v}$ (CFR. A_i.`Move`). In this heuristic, every agent's movement is done in feed-forward, as no localization is available yet.

Algorithm 2 `MovePolicy`

function MovePolicy(A_i) `Assumption:` $\mathcal{G}$ `connected at time` t_0
  if $\mathcal{N}_{i,RD} \neq \emptyset$ **then**
    if $\overline{\mathcal{N}}_{i,RD} \neq \emptyset$ **then** $\boldsymbol{v} \leftarrow A_i$.`DistGrad`$(\epsilon, \overline{\mathcal{N}}_{i,RD})$
    else $\boldsymbol{v} \leftarrow A_i$.`DistGrad`$(\epsilon, \mathcal{N}_{i,RD})$
    end if
  else $\boldsymbol{v} \leftarrow A_i$.`RandSelect`$(\mathcal{B}_\epsilon)$
  end if
  A_i.`Move`$(\boldsymbol{v})$
end function

Comments From algorithm 1 and algorithm 2, we see that the proposed procedure only considers the presence of neighbors for A_i; this is the only assumption we make, i.e., for $\mathcal{G}$ to be connected from the beginning. No rigidity assumption is required, differently from [35]. Connectivity is maintained during the exploration by discarding any movement $\boldsymbol{v}$ resulting in a neighbor loss. If this results in no feasible movement $\boldsymbol{v}$, A_i randomly chooses a feasible motion $\boldsymbol{v}$ in $\mathcal{B}_\epsilon$, similar to [35] (CFR. A_i.`RandSelect`). Specifically, $\boldsymbol{v}$ is feasible if a minimum distance $d_{\min}$ is kept between A_i and its neighbors. All these conditions are checked in A_i.`DistGrad`. Lastly, A_i.`ReduceFramework` complexity scales up with $|\overline{\mathcal{N}}^*_{i,RD}|$; thus, theorem 2 has been checked only on $\mathcal{F}^*$ such that $|\overline{\mathcal{N}}^*_{i,RD}| = |\overline{\mathcal{N}}_{i,RD}| - 1$.

4.2 The results

We prove the effectiveness of our solution by considering a batch of 100 randomly generated formations with $n = 8$ agents and the setup from section 2, where, for simplicity, the camera FOV is set to 360°. A single algorithm iteration consists of every agent A_i performing the three actions from section 4.1. The agents' sequence is randomly selected at every iteration. Figure 3 shows four frames of the algorithm execution on one of the formations. The algorithm succeeds if all the agents are localized after at most 200 iterations. Table 1 shows the success rate $\mathtt{S}_{\%}$, the average number of iterations $\mathtt{\#}_{\text{it}}$, and the coverage change $\mathtt{C} = \overline{C_0}/\overline{C_{\text{end}}}$ depending on $d_{\min}$ and ϵ. $\overline{C}$ is the average formation coverage. From the results, we see that increasing ϵ and reducing $d_{\min}$ results in higher performance and faster convergence due to the increased accuracy in the gradient computation and the higher number of feasible motions. The proposed algorithm successfully solves the network localization problem from section 2, with a coverage reduction of 20/25% as a side effect. We aim to address the coverage problem by reducing the formation contraction through the motion policy of the localized agents, which is currently not considered.

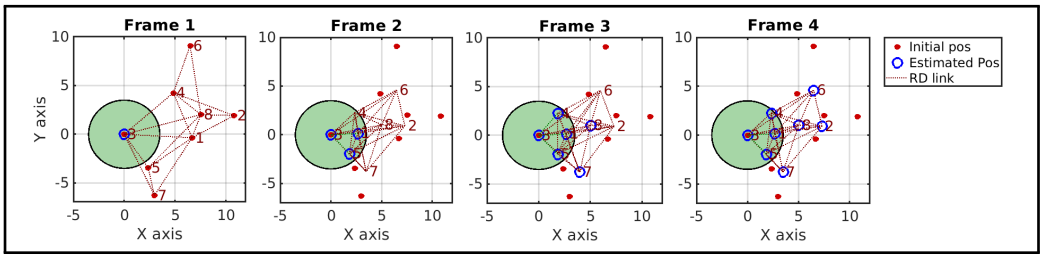

Fig. 3: Evolution of the solution to the network localization problem according to section 4.1. The green area around A_3 is the camera FOV.

ϵ \ $d_{\min}$	0.5m	1.0m	2.0m
0.25m	$\mathtt{S}_{\%} = 99, \#_{\text{it}} = 29.2, \mathtt{C} = 0.74$	$\mathtt{S}_{\%} = 96, \#_{\text{it}} = 30.7, \mathtt{C} = 0.75$	$\mathtt{S}_{\%} = 91, \#_{\text{it}} = 27.7, \mathtt{C} = 0.80$
0.50m	$\mathtt{S}_{\%} = 99, \#_{\text{it}} = 15.7, \mathtt{C} = 0.74$	$\mathtt{S}_{\%} = 97, \#_{\text{it}} = 15.9, \mathtt{C} = 0.77$	$\mathtt{S}_{\%} = 86, \#_{\text{it}} = 17.6, \mathtt{C} = 0.77$
0.75m	$\mathtt{S}_{\%} = 100, \#_{\text{it}} = 11.4, \mathtt{C} = 0.71$	$\mathtt{S}_{\%} = 98, \#_{\text{it}} = 10.7, \mathtt{C} = 0.75$	$\mathtt{S}_{\%} = 95, \#_{\text{it}} = 11.7, \mathtt{C} = 0.79$

Table 1: Algorithm performance on 100 formations depending on $d_{\min}$ and ϵ.

5 Rigidity spatial interpretation

This section studies how to exploit rigidity to address the environment coverage problem in the Active localization algorithm from section 4. From (1), reducing the overlapping areas I_{ij} increases the coverage. Generally speaking, to do so, increasing the team dispersion and symmetry is a reasonable policy. Thus, we analyze rigidity structural properties to understand whether exploiting it for coverage maximization is possible.

5.1 The analysis

For this analysis, we were first inspired by [36, 37], where the rigidity matrix properties are studied, proving a lemma equivalent to lemma 1:

Lemma 2 (Rigidity eigenvalue). *Consider a framework $(\mathcal{G}, \boldsymbol{p})$ in $\mathbb{R}^2$ with rigidity matrix $\mathcal{R} = \mathcal{R}(\mathcal{G}, \boldsymbol{p})$ from (3). Consider also the spectrum of the symmetric (positive semidefinite) rigidity matrix $\overline{\mathcal{R}} \triangleq \mathcal{R}^T\mathcal{R} \in \mathbb{R}^{2n\times 2n}$, i.e., the set of eigenvalues $0 \leq \lambda_1 \leq \ldots \lambda_{2n}$. If $(\mathcal{G}, \boldsymbol{p})$ is infinitesimally rigid, then $\lambda_i = 0\ \forall i \leq 3$.*

The first nonzero eigenvalue λ_4 is called *Worst-case Rigidity Index*[3] (WRI) in [36], and *rigidity eigenvalue*[4] in [37]. In both these papers, it is clearly shown that the greater λ_4, the higher the rigidity of the formation. However, [36] goes further, providing the following geometric interpretations:

[3]The name derives from the analogy between *rigidity* and *stiffness*; it describes the worst stress that the formation/structure can undergo without deforming.

[4]Zelazo considers the 3D case, where λ_4 is replaced by λ_7, due to the 6 roto-translations present in space. The reasoning does not change, though.

1. Increasing the connectivity between any pair of agents will always increase the formation's rigidity.
2. In general, the symmetry of the formation may positively impact the rigidity increase.

To better understand these intuitions, we consider the symmetric rigidity matrix $\overline{\mathcal{R}}$ for a framework $(\mathcal{G}, \boldsymbol{p})$, that can be written as

$$\overline{\mathcal{R}} = \begin{bmatrix} \sum\limits_{j\neq 1} a_1^j \mathrm{cov}(\boldsymbol{p}_1, \boldsymbol{p}_j) & -a_1^2 \mathrm{cov}(\boldsymbol{p}_1, \boldsymbol{p}_2) & \dots & -a_1^n \mathrm{cov}(\boldsymbol{p}_1, \boldsymbol{p}_n) \\ -a_2^1 \mathrm{cov}(\boldsymbol{p}_2, \boldsymbol{p}_1) & \sum\limits_{j\neq 2} a_2^j \mathrm{cov}(\boldsymbol{p}_2, \boldsymbol{p}_j) & \dots & -a_2^n \mathrm{cov}(\boldsymbol{p}_2, \boldsymbol{p}_n) \\ \vdots & \vdots & \vdots & \vdots \\ -a_n^1 \mathrm{cov}(\boldsymbol{p}_n, \boldsymbol{p}_1) & \dots & -a_n^{n-1} \mathrm{cov}(\boldsymbol{p}_n, \boldsymbol{p}_{n-1}) & \sum\limits_{j\neq n} a_n^j \mathrm{cov}(\boldsymbol{p}_n, \boldsymbol{p}_j) \end{bmatrix}, \tag{5}$$

where $\mathrm{cov}(\boldsymbol{p}_i, \boldsymbol{p}_j)$ is the covariance matrix[5] of a pair of agents. The scalar $a_i^j = a_j^i$ defines the presence or absence of a connection, i.e., $a_i^j \neq 0$, if and only if $j \in \mathcal{N}_i$. Thus, a framework described by a non-complete graph will have zero entries in $\overline{\mathcal{R}}$. If we further expand the structure of $\overline{\mathcal{R}}$, we find out that all the diagonal elements are nothing but the cumulative variances of all the neighbor sets $\mathcal{N}_i$, i.e., for a generic agent i, $\overline{\mathcal{R}}_{[2i-1,2i-1]} = \sum_{j\in\mathcal{N}_i} \sigma_x^2(\boldsymbol{p}_i, \boldsymbol{p}_j)$, and $\overline{\mathcal{R}}_{[2i,2i]} = \sum_{j\in\mathcal{N}_i} \sigma_y^2(\boldsymbol{p}_i, \boldsymbol{p}_j)$. If we consider the trace-eigenvalues property, we obtain:

$$\begin{aligned} \sum_i \lambda_i = \mathrm{tr}(\overline{\mathcal{R}}) &= \sum_i \sum_{j\in\mathcal{N}_i} \left(\sigma_x^2(\boldsymbol{p}_i, \boldsymbol{p}_j) + \sigma_y^2(\boldsymbol{p}_i, \boldsymbol{p}_j)\right) = \\ &= \sum_i \sum_{j\in\mathcal{N}_i} \left((p_{i,x} - p_{j,x})^2 + (p_{i,y} - p_{j,y})^2\right) \geq 0. \end{aligned} \tag{6}$$

From (6), we see that maximizing the inter-agent variances, namely spreading the formation, increases the eigenvalues of $\overline{\mathcal{R}}$. It is also clear that more connections generally yield a higher trace. However, (6) does not directly imply that a higher trace means higher λ_4. Furthermore, in [36], no maximum detection range is considered between agents; here, we consider a more realistic case where $a_i^j \neq 0$ if $\|\boldsymbol{p}_i - \boldsymbol{p}_j\| < \delta$, in accordance with our case study. In this situation, we might have different configurations maximizing the framework's eigenvalues, either with more connections or higher dispersion. We will numerically investigate these aspects in section 5.2.

We proceed by considering symmetry in the formation. We first note that (5) describes $\overline{\mathcal{R}}$ as a block matrix, the blocks being the inter-agent covariance matrices and their summation. Indeed, the eigenvalues of $\overline{\mathcal{R}}$ depend on its determinant, which nonlinearly depends too on $\det(\mathrm{cov}(\boldsymbol{p}_i, \boldsymbol{p}_j))$. We are not interested in this exact relation but rather in the intuition that $\det(\overline{\mathcal{R}})$ will depend on a variance-related and a covariance-related term, similar to a generic covariance matrix determinant:

$$\det(\mathrm{cov}(\boldsymbol{p})) = (\sigma_x^2 + \sigma_y^2) - \sigma_{xy}^2 \implies \det(\overline{\mathcal{R}}) \propto \gamma_D(\sigma_x^2, \sigma_y^2) + \gamma_S(\sigma_{xy}), \tag{7}$$

[5] We normalized the terms, i.e., for a pair of agents, we multiplied by 2 the matrix.

with γ_D, γ_S continuous maps, and the variance and covariance terms defined as

$$\sigma^2_{x/y} \triangleq \frac{1}{n}\sum_{i=1}^{n}\left(p_{i,x/y} - \frac{1}{|\mathcal{N}_i|}\sum_{j\in\mathcal{N}_i} a_i^j p_{j,x/y}\right)^2, \tag{8a}$$

$$\sigma_{xy} \triangleq \frac{1}{n}\sum_{i=1}^{n}\left(p_{i,x} - \frac{1}{|\mathcal{N}_i|}\sum_{j\in\mathcal{N}_i} a_i^j p_{j,x}\right)\left(p_{i,y} - \frac{1}{|\mathcal{N}_i|}\sum_{j\in\mathcal{N}_i} a_i^j p_{j,y}\right). \tag{8b}$$

From standard statistics, we know that $\sigma_{xy} = \rho\sigma_x\sigma_y$, where ρ is the correlation coefficient. For a pair of agents $\rho = \pm 1$, but for the whole formation, maximizing σ^2_{xy} means placing the agents of a neighborhood $\mathcal{N}_i$ on a straight line ($\rho^2 \to 1$) while minimizing it means obtaining a symmetric formation ($\rho^2 \to 0$). We will further investigate this aspect through numerical simulations in section 5.2.

This analysis showed how the symmetric rigidity matrix $\overline{\mathcal{R}}$ and the inter-agent covariance matrices $\mathrm{cov}(\boldsymbol{p}_i, \boldsymbol{p}_j)$ share the same underlying structure. Exploiting this analogy, we analytically support the intuitions from [36] regarding the effects of connectivity and symmetry on a formation's rigidity. Furthermore, we also relate rigidity with the spatial dispersion of the framework. In the next section, we investigate these results through numerical simulations.

5.2 The results

This section investigates the results from section 5.1 through numerical simulations, considering the setup from section 2. We also add a constraint on the minimum distance between agents to avoid collisions, mimicking the outcome of the motion policy proposed in section 4.

Dispersion and connectivity We study how the trace-eigenvalues relation from (6) affects the formation dispersion and connectivity and its relation to the rigidity eigenvalue λ_4. To do so, we consider the following optimization problems:

$$\begin{aligned} \min_{(\mathcal{G},\boldsymbol{p})} \quad & -\mathrm{tr}(\overline{\mathcal{R}}) \\ \text{s.t.} \quad & \lambda_4 > 0 \\ & d_{\min} \le d_{ij} \le d_{\max} \le \delta \end{aligned} \tag{9a}$$

$$\begin{aligned} \min_{(\mathcal{G},\boldsymbol{p})} \quad & -\lambda_4 \\ \text{s.t.} \quad & \lambda_4 > 0 \\ & d_{\min} \le d_{ij} \le d_{\max} \le \delta \end{aligned} \tag{9b}$$

where framework $(\mathcal{G}, \boldsymbol{p})$ is constrained the to be rigid. The collision safety condition is represented by the $d_{\min} \le d_{ij}$ constraint. The $d_{ij} \le d_{\max}$ condition manually limits the dispersion of the team. By solving (9a) and (9b), the question that we are addressing is: *among all the rigid frameworks with a minimum and a maximum inter-agent distance, does maximum rigidity coincide with either maximum connectivity or dispersion?*

In fig. 4, we show the results of a three batch of simulations set for $n = 4$ agents: problems (9a) (left-side) and (9b) (right-side) were solved with $d_{\min} = \{1, 2, 3\}$ m, and with $d_{\max} \in [d_{\min} + 1,\ \delta]$. In the top plots, we show $\mathrm{tr}(\overline{\mathcal{R}})$, in the middle λ_4, and in the bottom the number of connections among agents. We first note that for every $d_{\min}$, the optimization objectives monotonically increase

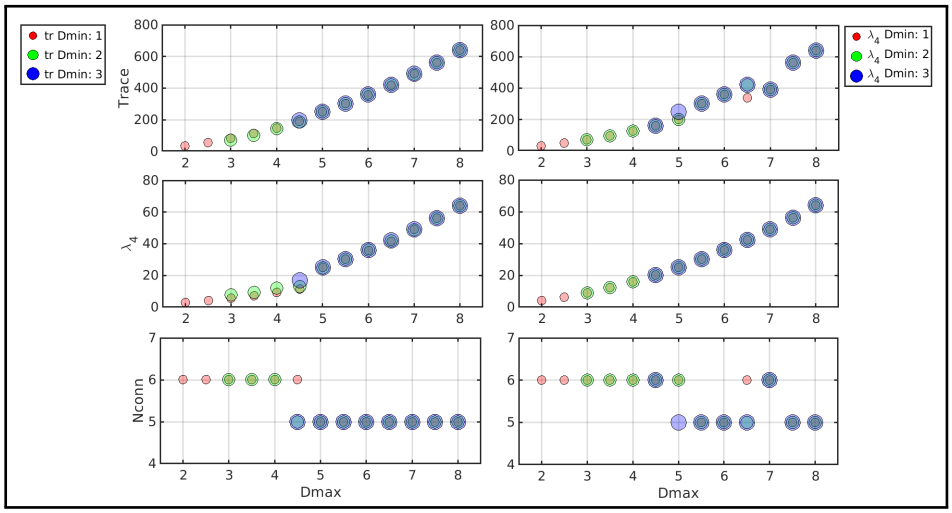

Fig. 4: Numerical solutions to (9a) and (9b) under different sets of constraints.

with $d_{\max}$ (CFR. top-left and mid-right). As for λ_4, these simulations show that dispersion does have a positive impact on rigidity. However, as expected, maximizing either connectivity or dispersion does not imply maximizing rigidity, as highlighted by the mid-left and top-right plots, which show different behaviors than the optimization objectives. Lastly, if we look at the number of connections (CFR. bottom plots), the general trend is to prefer dispersion over connectivity as $d_{\max}$ increases. However, this is not an absolute behavior, showing cases where connectivity helps rigidity more than dispersion [36]. It is clear, though, that, if combined, these two factors always help to increase λ_4.

Simmetry We now analyze the rigidity-symmetry relation provided in section 5.1 by considering again (9b) together with the following problems:

$$\begin{aligned} \min_{(\mathcal{G},\boldsymbol{p})} \quad & -\lambda_4 + \rho^2 \\ \text{s.t.} \quad & \lambda_4 > 0 \\ & d_{\min} \leq d_{ij} \leq d_{\max} \leq \delta \end{aligned} \tag{10a}$$

$$\begin{aligned} \min_{(\mathcal{G},\boldsymbol{p})} \quad & -\lambda_4 \\ \text{s.t.} \quad & \lambda_4 > 0 \\ & d_{\min} \leq d_{ij} \leq d_{\max} \leq \delta \\ & |\rho| \geq 0.5 \end{aligned} \tag{10b}$$

Specifically, we address the following questions: *does rigidity maximization directly take into account symmetry maximization? Is it true that lower symmetry, in general, implies lower rigidity?*

In fig. 5, we show the solutions to (9b),(10a),(10b) for $n = 4$ (left-side), and $n = 5$ (right-side) agents. In the top plots, we show ρ^2, and in the bottom, λ_4. If we consider (9b) and (10a), we observe that the cost function values almost coincide; thus, optimizing on rigidity already comprehend maximizing symmetry.

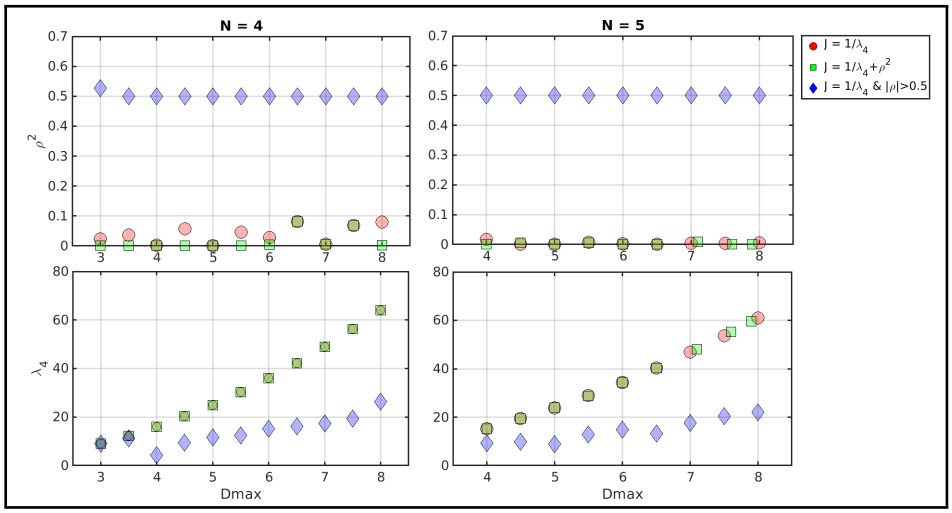

Fig. 5: Numerical solutions to (9b),(10a),(10b) under constraints and agents' number.

If we force a minimum $|\rho|$ value, it is pretty clear that rigidity worsens; thus, it is true that lower rigidity generally implies lower symmetry.

This section provided an analytical interpretation of rigidity; we showed through extensive numerical simulations that increasing rigidity results in higher formation symmetry, dispersion, and hence higher coverage. Thus, the algorithm from section 4 can be extended by moving the localized agents to maximize λ_4, again maintaining connectivity. This will reduce the formation contraction, addressing the coverage problem as initially proposed. We will analyze this solution further in future works.

6 Conclusions and future work

In this work we addressed the joint Active localization and exploration coverage problem for heterogenous teams organized with one leader and a set of children. Firstly, in section 4, we solved the network localization problem in the leader's reference frame in a distributed manner through Rigidity Theory. Then, in section 5 we analytically interpreted rigidity in terms of the team's dispersion, symmetry, and connectivity. Specifically, we showed that the team's coverage can be maximized through rigidity. We concluded by proposing an extension of the Active localization algorithm which maximizes the team's coverage. We will further proceed in this direction implementing the rigidity-based coverage maximization in the Active localization algorithm from section 4.

Acknowledgements We would like to express our sincere gratitude to Karen-Lee Bar-Sinai, Tom Shaked, Bhaskar Vundurthy, Geordan Gutow, and Howie Choset for their valuable contributions to this work.

References

1. Yara Rizk, Mariette Awad, and Edward W. Tunstel. Cooperative Heterogeneous Multi-Robot Systems: A Survey. *ACM Computing Surveys*, 2019.
2. Alan Mainwaring, David Culler, Joseph Polastre, Robert Szewczyk, and John Anderson. Wireless sensor networks for habitat monitoring. In *Proceedings of the 1st ACM international workshop on Wireless sensor networks and applications*, 2002.
3. Liyang Yu, Neng Wang, and Xiaoqiao Meng. Real-time forest fire detection with wireless sensor networks. In *Proceedings. 2005 International Conference on Wireless Communications, Networking and Mobile Computing, 2005.*, 2005.
4. John B. Folkesson and Henrik I. Christensen. Robust SLAM. *IFAC Proceedings Volumes*, 2004.
5. Ragesh K Ramachandran, Sean Wilson, and Spring Berman. A probabilistic topological approach to feature identification using a stochastic robotic swarm. In *Distributed Autonomous Robotic Systems: The 13th International Symposium*, pages 3–16. Springer, 2018.
6. Farid Bounini, Denis Gingras, Hervé Pollart, and Dominique Gruyer. From Simultaneous Localization and Mapping to Collaborative Localization for Intelligent Vehicles. *IEEE Intelligent Transportation Systems Magazine*, 2021.
7. Sarah Brent, Chengzhi Yuan, and Paolo Stegagno. Swarm localization through cooperative landmark identification. In *Distributed Autonomous Robotic Systems: 15th International Symposium*, pages 429–441. Springer, 2022.
8. Usman A. Khan, Soummya Kar, and JosÉ M. F. Moura. Distributed Sensor Localization in Random Environments Using Minimal Number of Anchor Nodes. *IEEE Transactions on Signal Processing*, 2009.
9. Sam Safavi, Usman A. Khan, Soummya Kar, and José M. F. Moura. Distributed Localization: A Linear Theory. *Proceedings of the IEEE*, 2018.
10. Michiaki Hirayama, Alicja Wasik, Mitsuhiro Kamezaki, and Alcherio Martinoli. Robust localization for multi-robot formations: An experimental evaluation of an extended gm-phd filter. In *Distributed Autonomous Robotic Systems: 15th International Symposium*, pages 148–162. Springer, 2022.
11. RA Thivanka Perera, Chengzhi Yuan, and Paolo Stegagno. A phd filter based localization system for robotic swarms. In *Distributed Autonomous Robotic Systems: 15th International Symposium*, pages 176–189. Springer, 2022.
12. Teemu Roos, Petri Myllymäki, Henry Tirri, Pauli Misikangas, and Juha Sievänen. A Probabilistic Approach to WLAN User Location Estimation. *International Journal of Wireless Information Networks*, 2002.
13. Stefano Maranò, Wesley M. Gifford, Henk Wymeersch, and Moe Z. Win. NLOS identification and mitigation for localization based on UWB experimental data. *IEEE Journal on Selected Areas in Communications*, 2010.
14. Anwar Quraishi and Alcherio Martinoli. Distributed cooperative localization with efficient pairwise range measurements. In *Distributed Autonomous Robotic Systems: 15th International Symposium*, pages 134–147. Springer, 2022.
15. Kihoon Shin, Hyunjae Sim, Seungwon Nam, Yonghee Kim, Jae Hu, and Kwang-Ki K. Kim. Multi-Robot Relative Pose Estimation in SE(2) with Observability Analysis: A Comparison of Extended Kalman Filtering and Robust Pose Graph Optimization, 2024.
16. Shota Tanaka, Takahiro Endo, and Fumitoshi Matsuno. Decentralized navigation in 3d space of a robotic swarm with heterogeneous abilities. In *Distributed Autonomous Robotic Systems: 15th International Symposium*, pages 389–400. Springer, 2022.

17. Julio A. Placed, Jared Strader, Henry Carrillo, Nikolay Atanasov, Vadim Indelman, Luca Carlone, and José A. Castellanos. A Survey on Active Simultaneous Localization and Mapping: State of the Art and New Frontiers. *IEEE Transactions on Robotics*, 2023.
18. R. Kurazume, S. Nagata, and S. Hirose. Cooperative positioning with multiple robots. In *Proceedings of the 1994 IEEE International Conference on Robotics and Automation*, 1994.
19. R. Kurazume, S. Hirose, S. Nagata, and N. Sashida. Study on cooperative positioning system (basic principle and measurement experiment). In *Proceedings of IEEE International Conference on Robotics and Automation*, 1996.
20. R. Kurazume and S. Hirose. Study on cooperative positioning system: optimum moving strategies for CPS-III. In *Proceedings. 1998 IEEE International Conference on Robotics and Automation (Cat. No.98CH36146)*, 1998.
21. B. Yamauchi, A. Schultz, and W. Adams. Mobile robot exploration and map-building with continuous localization. In *Proceedings. 1998 IEEE International Conference on Robotics and Automation (Cat. No.98CH36146)*, May 1998.
22. J. Spletzer, A.K. Das, R. Fierro, C.J. Taylor, V. Kumar, and J.P. Ostrowski. Cooperative localization and control for multi-robot manipulation. In *Proceedings 2001 IEEE/RSJ International Conference on Intelligent Robots and Systems. Expanding the Societal Role of Robotics in the the Next Millennium (Cat. No.01CH37180)*. IEEE, 2001.
23. Bruce Hendrickson. Conditions for Unique Graph Realizations. *SIAM Journal on Computing*, 1992.
24. T. Eren, O.K. Goldenberg, W. Whiteley, Y.R. Yang, A.S. Morse, B.D.O. Anderson, and P.N. Belhumeur. Rigidity, computation, and randomization in network localization. In *IEEE INFOCOM 2004*, 2004.
25. J. Aspnes, T. Eren, D.K. Goldenberg, A.S. Morse, W. Whiteley, Y.R. Yang, B.D.O. Anderson, and P.N. Belhumeur. A Theory of Network Localization. *IEEE Transactions on Mobile Computing*, 2006.
26. Alyxander Burns, Bernd Schulze, and Audrey St. John. Persistent multi-robot formations with redundancy. In *Distributed Autonomous Robotic Systems: The 13th International Symposium*, pages 133–146. Springer, 2018.
27. Daniel Zelazo, Paolo Robuffo Giordano, and Antonio Franchi. Bearing-only formation control using an SE(2) rigidity theory. In *2015 54th IEEE Conference on Decision and Control (CDC)*, 2015.
28. Shiyu Zhao and Daniel Zelazo. Bearing Rigidity and Almost Global Bearing-Only Formation Stabilization. *IEEE Transactions on Automatic Control*, 2016.
29. Shiyu Zhao and Daniel Zelazo. Bearing Rigidity Theory and Its Applications for Control and Estimation of Network Systems: Life Beyond Distance Rigidity. *IEEE Control Systems Magazine*, 2019.
30. Giulia Michieletto, Angelo Cenedese, and Daniel Zelazo. A Unified Dissertation on Bearing Rigidity Theory. *IEEE Transactions on Control of Network Systems*, 8, 2021.
31. Luciano C. A. Pimenta, Vijay Kumar, Renato C. Mesquita, and Guilherme A. S. Pereira. Sensing and coverage for a network of heterogeneous robots. In *2008 47th IEEE Conference on Decision and Control*, 2008.
32. Luca Giuggioli, Idan Arye, Alexandro Heiblum Robles, and Gal A Kaminka. From ants to birds: A novel bio-inspired approach to online area coverage. In *Distributed Autonomous Robotic Systems: The 13th International Symposium*, pages 31–43. Springer, 2018.

33. Guillaume Sartoretti, Ananya Rao, and Howie Choset. Spectral-based distributed ergodic coverage for heterogeneous multi-agent search. In *International Symposium Distributed Autonomous Robotic Systems*, pages 227–241. Springer, 2021.
34. Ayan Dutta, O Patrick Kreidl, and Jason M O'Kane. Opportunistic multi-robot environmental sampling via decentralized markov decision processes. In *Distributed Autonomous Robotic Systems: 15th International Symposium*, pages 163–175. Springer, 2022.
35. Iman Shames, Tyler H. Summers, Farhad Farokhi, and Rohan C. Shekhar. Conditions and strategies for uniqueness of the solutions to cooperative localization and mapping problems using rigidity theory. In *2015 54th IEEE Conference on Decision and Control (CDC)*, 2015.
36. Guangwei Zhu and Jianghai Hu. Stiffness matrix and quantitative measure of formation rigidity. In *Proceedings of the 48h IEEE Conference on Decision and Control (CDC) held jointly with 2009 28th Chinese Control Conference*, 2009.
37. Daniel Zelazo, Antonio Franchi, Heinrich H. Bülthoff, and Paolo Robuffo Giordano. Decentralized rigidity maintenance control with range measurements for multi-robot systems. *The International Journal of Robotics Research*, 2015.
38. David Moore, John Leonard, Daniela Rus, and Seth Teller. Robust distributed network localization with noisy range measurements. In *Proceedings of the 2nd international conference on Embedded networked sensor systems*, 2004.